

**Photoinduced giant magnetic polarons in EuTe**A. B. Henriques,<sup>1</sup> A. R. Naupa,<sup>1</sup> P. A. Usachev,<sup>2</sup> V. V. Pavlov,<sup>2</sup> P. H. O. Rappl,<sup>3</sup> and E. Abramof<sup>3</sup><sup>1</sup>*Instituto de Física, Universidade de Sao Paulo, 05315-970 Sao Paulo, Brazil*<sup>2</sup>*Ioffe Institute, 194021 St. Petersburg, Russia*<sup>3</sup>*LAS-INPE, 12227-010 Sao Jose dos Campos, Brazil*

(Received 8 October 2016; published 13 January 2017)

Photoinduced magnetic polarons in EuTe, with a magnetic moment of several hundred Bohr magnetons, were investigated as a function of pump intensity and temperature by pump-probe Faraday rotation. The quantum efficiency for optical generation of magnetic polarons is found to be 0.09. The pump-intensity dependence of the photoinduced Faraday rotation shows a sublinear increase, from which we deduce that the population of photoexcited polarons is limited by a maximum value of  $4.5 \times 10^{15} \text{ cm}^{-3}$ . This is four orders of magnitude less than the concentration of polarons that would completely fill the crystal, which suggests that the photoexcited polarons are anchored by defects. In addition to the generation of polarons, at high pump densities the modulated pump light also causes a small alternating heating of the illuminated region. The temperature dependence of the polaron magnetic moment is well described by the Curie–Weiss law. Above 100 K, polarons are thermally quenched with an activation energy of 11 meV.

DOI: [10.1103/PhysRevB.95.045205](https://doi.org/10.1103/PhysRevB.95.045205)

Optical manipulation of the magnetic state of matter is a topic of current interest both from the fundamental point of view as well as due to its high relevance in respect to technological applications [1]. Magnetic semiconductors represent a family of materials with a huge potential for fast optomagnetism [2–4], yet they remain largely unexplored in respect to optical manipulation of their magnetic state. Europium telluride is an intrinsic magnetic semiconductor of the face-centered cubic structure, where an europium spin  $S = 7/2$  is associated with every lattice site. EuTe is an antiferromagnet with a Néel temperature of  $T_N = 9.6 \text{ K}$ , hence its equilibrium magnetization is zero. Recently it was demonstrated that in EuTe light in resonance with the band gap can generate magnetic polarons with a magnetic moment of several hundred Bohr magnetons at temperatures as high as 100–150 K [5–7]. A magnetic polaron consists of a conduction-band electron localized in space by a photoexcited hole and the attractive exchange field generated by the spins of the europium atoms within the range of the electronic wave function. Magnetic polarons have been widely studied in diluted magnetic semiconductors (see, for instance, Refs. [8,9]). In intrinsic magnetic semiconductors, the theory of magnetic polarons was first studied by Kasuya and Nagaev [10,11]. A variational approximation to describe magnetic polarons is described in Ref. [12]. In Ref. [6], the more sophisticated self-consistent field approximation was used, and the theory was used to extract magnetic polaron parameters from the EuTe low temperature photoluminescence, which was measured as a function of applied magnetic field. It was found that, for EuTe, the magnetic polaron is described by a sphere of radius  $R_{\text{Pol}} \approx 4$  (in units of the EuTe lattice parameter), which is nearly independent of temperature and field, and the magnetic moment of the polaron is  $\sim 610 \mu_B$  below the Néel temperature [5,6]. Because of the giant magnetic moment of a polaron, a modest magnetic field of a few tens of mT leads to a full alignment of polarons, which opens the prospect of using light to magnetize EuTe. To determine how efficiently this light magnetization mechanism can be exploited, here we investigate photoinduced magnetic polarons

in EuTe as a function of pump intensity and temperature by using pump-probe Faraday rotation.

The EuTe sample was grown by molecular beam epitaxy (MBE) on a (111)-oriented BaF<sub>2</sub> substrate [13]. The thickness of the EuTe epitaxial layer was  $d_{\text{Sample}} = 1.3 \mu\text{m}$ , and the epitaxial layer was capped with BaF<sub>2</sub> to ensure total protection of the EuTe surface from oxidation. The thickness of the protective layer was 200 nm. BaF<sub>2</sub> is completely transparent in the wavelength range used in this paper, therefore the thickness of the protective layer is not critical for the present study. The photoinduced Faraday rotation (PFR) was measured by using a two-color pump-probe technique. The pump light source was a frequency-doubled Nd:YAG laser (2.33 eV), focused on the sample with a Gaussian profile of 150  $\mu\text{m}$  full width at half maximum. The Faraday rotation probe was a semiconductor laser of photon energy 1.86 eV. This photon energy is well within the EuTe gap for any field and temperature used in our measurements, so the probe is not absorbed. Therefore it does not photoexcite any electron-hole pairs, and hence it does not induce any magnetic polarons (the photoinduced magnetic polaron excitation spectrum is given in Ref. [7]). A magnetic field was applied normal to the surface of the sample, which is parallel to the [111] crystalline direction. The experiments were performed using a variable-temperature optical cryostat containing a superconductive coil to generate a magnetic field applied in the Faraday geometry. The pump was modulated at 2.33 kHz using a chopper. The Faraday rotation angle of the linearly polarized probe beam was measured by using a polarization bridge containing a New Focus Nirvana balanced detector coupled to a lock-in referenced to the chopper frequency [14].

The Faraday rotation angle  $\theta_F$  of the light that crosses a uniformly magnetized sample of thickness  $d_{\text{Sample}}$  can be converted into its magnetization  $M$  by using [15]

$$\theta_F = V M d_{\text{Sample}}, \quad (1)$$

where  $V$  is the Verdet constant. The Verdet constant at the probe wavelength was determined from a measurement of the Faraday rotation of the probe light, at 5 K, as a function

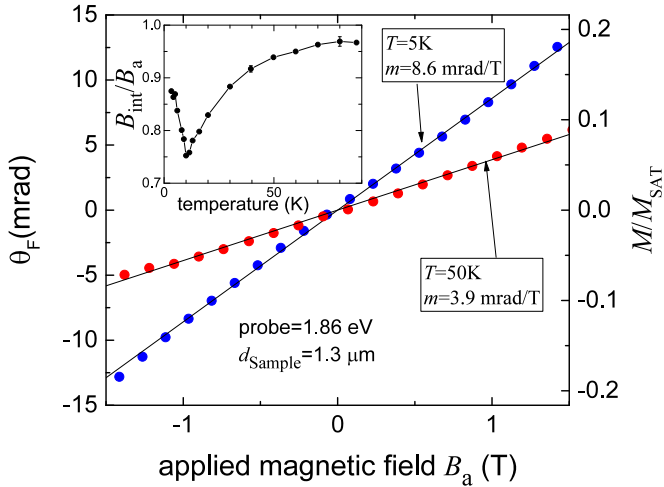


FIG. 1. Faraday rotation by the bulk EuTe sample as a function of the applied magnetic field at  $T = 5$  K and  $T = 50$  K. The inset shows the ratio of the internal magnetic field to the applied magnetic field.

of the applied magnetic field. During this measurement the pump light was switched off. To isolate the EuTe Faraday rotation signal, the contribution coming from the cryostat windows was subtracted. As expected, we found that the photoinduced Faraday rotation is independent of the intensity of the probe because the probe used is well within the EuTe transparency-wavelength range. As shown in Fig. 1, the Faraday rotation depends linearly on applied field  $B_a$  with a slope of  $m(T = 5 \text{ K}) = 8.6 \text{ mrad/T}$ . At  $T = 5$  K the magnetization is also linear in  $B_a$ , with a slope of  $M_{\text{SAT}}/B_{\text{SAT}}$  [16], where  $M_{\text{SAT}} = n_{\text{Eu}}\mu_{\text{Eu}} = 9.03 \times 10^5 \text{ A/m}$  is the saturation magnetization, where  $n_{\text{Eu}} = 4/a^3$  is the concentration of Eu atoms in the fcc lattice of parameter  $a = 6.6 \text{ \AA}$ ,  $\mu_{\text{Eu}} = g\mu_B S$  is the magnetic moment of an Eu atom,  $g = 2$  is the  $\text{Eu}^{2+}$  gyromagnetic factor,  $\mu_B$  is the Bohr magneton, and  $B_{\text{SAT}} = 8.3 \text{ T}$  is the saturation field in the Faraday geometry [16]. Hence the Verdet constant, for the probe wavelength  $\lambda = 665 \text{ nm}$ , is found to be

$$V = \frac{B_{\text{SAT}}m(T = 5 \text{ K})}{d_{\text{Sample}}M_{\text{SAT}}} = 0.061 \text{ rad/A.} \quad (2)$$

Being determined by the electronic energy structure, the Verdet constant will remain approximately constant as a function of temperature and magnetic field, as long as the electronic energy structure and the band gap are not modified. It is well known that the EuTe band gap changes when the lattice spins are strongly polarized, but this requires magnetic fields above 3 T at helium temperatures (see, for instance, Figs. 4 and 5 in Ref. [17]), and proportionally larger fields at higher temperatures. Because the magnetic fields used here are modest in comparison, we can safely assume, to a good approximation, that the Verdet constant is independent of temperature and magnetic field for all the experimental results presented here.

In addition to converting a Faraday rotation angle to magnetization, the Verdet constant also allows us to determine the internal magnetic field, which is smaller than the applied one due to the demagnetization field. In the Faraday geometry

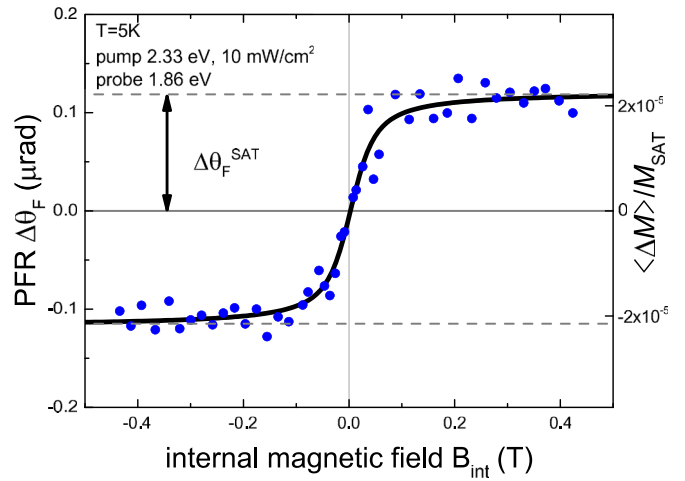


FIG. 2. Photoinduced Faraday rotation (PFR) signal as a function of the internal magnetic field at  $T = 5$  K.

used, the demagnetization field within the epitaxial layer is given by  $\mu_0 M$  [18], hence the internal magnetic field will be given by

$$B_{\text{int}} = B_a - \mu_0 M. \quad (3)$$

Substituting  $M$  from Eq. (1), and using  $\theta_F = m(T)B_a$ , where  $m(T)$  is the slope of the Faraday rotation angle as a function of  $B_a$  at a temperature  $T$  (see Fig. 1), then the ratio  $B_{\text{int}}/B_a$  will be given by

$$\frac{B_{\text{int}}}{B_a} = 1 - \mu_0 \frac{m(T)}{d_{\text{Sample}}V}. \quad (4)$$

The ratio  $B_{\text{int}}/B_a$ , calculated by using Eq. (4), is plotted in the inset of Fig. 1 as a function of temperature. The sharp downfall of the  $B_{\text{int}}/B_a$  ratio in the vicinity of 10 K is because EuTe is an antiferromagnet, therefore its temperature-dependent magnetic susceptibility shows the characteristic cusp at the Néel temperature (see, for instance, Ref. [19]). Therefore, according to Eq. (3), the absolute value of the internal field  $B_{\text{int}}$  is expected to show a corresponding downward cusp at the Néel temperature, as indeed observed in the inset of Fig. 1.

By using the results of the preceding preliminary analysis, we can convert the measured photoinduced Faraday rotation, as a function of *applied* magnetic field  $B_a$  into photoinduced magnetization as a function of the *internal* magnetic field  $B_{\text{int}}$ . Figure 2 shows the photoinduced Faraday rotation signal (PFR) at 5 K as a function of the internal field for a pump intensity of  $10 \text{ mW/cm}^2$ . The photoinduced Faraday rotation angle was converted into magnetization by using the Verdet constant determined above and assuming that the thickness  $d_{\text{pol}}$  of the layer where magnetic polarons are photogenerated is equal to the pump-light penetration depth  $1/\alpha$ , i.e.,  $d_{\text{pol}} = \frac{1}{\alpha}$ , where  $\alpha = 10 \text{ \mu m}^{-1}$  is the absorption coefficient at the pump wavelength [17]. The photoinduced magnetization scale obtained in this way is shown on the right-hand side of Fig. 2.

The photoinduced Faraday rotation signal shown in Fig. 2 has all the characteristics expected for an ensemble of photoexcited polarons. First, the signal shows a resonance

when the energy of the pump photons meets the EuTe band gap [7]. Second, the signal is zero at  $B = 0$ , because at  $B = 0$  there is no preferential direction in space, therefore photoexcited magnetic polarons will point randomly, and the net magnetic moment of the sample will remain zero. Third, the photoinduced signal tends to saturate rapidly when a magnetic field is applied, exactly as expected for magnetic polarons of a large magnetic moment—several hundreds of Bohr magnetons.

Assuming that the photoexcited polarons do not diffuse, the saturation value of the photoinduced Faraday rotation seen in Fig. 2,  $\Delta\theta_F^{\text{SAT}} = 0.12 \mu\text{rad}$ , can be converted to an average photoinduced magnetization

$$\langle\Delta M\rangle^{\text{SAT}} = \frac{\alpha\Delta\theta_F^{\text{SAT}}}{V} = 2.2 \times 10^{-5} M_{\text{SAT}}. \quad (5)$$

This value can be compared with the value expected for photoinduced polarons

$$\langle\Delta M\rangle^{\text{SAT}} = n_{\text{Pol}}\mu_{\text{Pol}}, \quad (6)$$

where  $\mu_{\text{Pol}} \sim 610\mu_B$  is the magnetic moment of a polaron at 5 K [5,6], and  $n_{\text{Pol}}$  is the steady-state population of magnetic polarons when the sample is illuminated with the pump light. The inertial effective mass of a magnetic polaron has been predicted to increase exponentially with the ratio of the polaron radius and the lattice parameter,  $R_{\text{Pol}}/a$  [20]. Because in our case this ratio is quite large,  $R_{\text{Pol}}/a \sim 4$  [6], we expect the photoinduced magnetic polarons to be quite heavy and immobile, and they therefore remain in the layer penetrated by the pump light. In this case the steady-state polaron population will be given by  $n_{\text{Pol}} = G\tau_0$ , where  $G$  is the polaron average generation rate per unit volume within the light penetration depth  $1/\alpha$ ,  $G = \chi \frac{p\alpha}{h\nu}$ ,  $p$  is the intensity of the pump beam incident on the surface of the sample,  $\chi$  is the quantum efficiency of polaron generation,  $h\nu$  is the pump photon energy, and  $\tau_0 = 15 \mu\text{s}$  is the polaron lifetime at  $T = 5 \text{ K}$  [7]. All parameters determining  $\langle\Delta M\rangle^{\text{SAT}}$  are known, except for the quantum efficiency, so a comparison of Eqs. (5) and (6) yields the quantum efficiency  $\chi \approx 0.09$ . This result is very reasonable and can be taken as further evidence that photoinduced magnetic polarons are the source of the photoinduced Faraday rotation signal observed.

By using the deduced quantum efficiency, the steady-state polaron population is found to be  $n_{\text{Pol}} = 3.6 \times 10^{15} \text{ cm}^{-3}$ . Therefore the average distance between polarons is estimated to be  $d = 2(\frac{3}{4\pi n_{\text{Pol}}})^{1/3} \sim 120a$ , where  $a$  is the EuTe lattice parameter. Taking into account that the radius of a polaron is  $R_{\text{Pol}} \sim 4a$  [6], then the distance between polarons is two orders of magnitude greater than the polaron radius, hence it can be assumed that polarons are noninteracting.

Having firmly established that the photoinduced Faraday rotation signal is due to optically generated magnetic polarons, that these polarons are very distant from one another, and knowing that the magnetic moment of a polaron equals several hundreds of Bohr magnetons [5,6], we can conjecture that the magnetization of a magnetic polaron ensemble will obey a Langevin function, which describes a paramagnetic system in the classical limit. In this hypothesis the magnetization associated with a photoinduced magnetic polaron ensemble

will be given by

$$\langle\Delta M(B, T)\rangle = n_{\text{Pol}}\mu_{\text{Pol}}L(x), \quad (7)$$

where the Langevin function is given by

$$L(x) = \coth(x) - \frac{1}{x}, \quad (8)$$

where  $x = \frac{\mu_{\text{Pol}}B}{k_B T}$ . Notice that, below the Néel temperature, the magnetic moment of the polaron is known from photoluminescence studies to be  $610\mu_B$  [5,6], hence in that temperature range there are no free parameters in Eq. (7). Nevertheless, to test the validity of our Langevin conjecture, we have fitted the photoinduced magnetization data taken at  $T = 5 \text{ K}$  with Eq. (7), whereby the polaron magnetic moment is the sole adjustable parameter. The fitted curve is depicted by the solid line in Fig. 2, yielding  $\mu_{\text{Pol}} \sim 600\mu_B$ . This coincides almost exactly with the known value, which demonstrates that the magnetization of the photoinduced magnetic polaron ensemble indeed follows a Langevin function.

Next we investigate the possibility of generating a higher population of photoinduced polarons by increasing the pump intensity. Figure 3(a) shows the dependence of the PFR as a function of pump intensity for  $T = 5 \text{ K}$ . As the pump intensity is increased, a linear background appears, whose slope is proportional to the pump intensity, suggesting a heating effect. A temperature increase of the bulk by  $\Delta T$  will cause a change in its magnetization by

$$\Delta M = \frac{\partial M}{\partial T} \Delta T. \quad (9)$$

Here  $\Delta M$  represents the change in magnetization due to sample heating within the pump-light penetration depth  $d_{\text{Pol}} = \frac{1}{\alpha}$ , which from Eq. (1) is given by

$$\Delta M = \frac{\Delta\theta_F}{V d_{\text{Pol}}}. \quad (10)$$

Similarly,  $\frac{\partial M}{\partial T}$  is also related to the bulk Faraday rotation,

$$\frac{\partial M}{\partial T} = \frac{1}{V d_{\text{Sample}}} \frac{\partial\theta_F}{\partial T}. \quad (11)$$

At fields sufficiently large, when the polaron magnetization is saturated, only a thermal effect can contribute to the slope of  $\Delta M$ . Therefore, substituting Eqs. (10) and (11) in Eq. (9), and resolving for  $\Delta T$ , we get

$$\Delta T = \frac{d_{\text{Sample}}}{d_{\text{Pol}}} \frac{\text{slope of } \Delta\theta_F \text{ at high fields}}{\text{slope of } \frac{\partial\theta_F}{\partial T}}, \quad (12)$$

where the slope of  $\frac{\partial\theta_F}{\partial T}$  was taken from the inset of Fig. 3(c), and the slope of  $\Delta\theta_F$  was taken from the high-field limit in Figs. 3(a) and 3(b).

The temperature increase  $\Delta T$  calculated from Eq. (12) is shown as a function of the pump intensity in Fig. 3(d). Our interpretation in terms of a heating effect is confirmed by the photoinduced Faraday rotation curves as a function of intensity, done at a temperature of 50 K [Fig. 3(b)]. Because for EuTe the Faraday rotation dependence has the typical behavior of an antiferromagnet, with a maximum at the Néel temperature [see Fig. 3(c)], the slope of the thermal background seen in the PFR signal should change from positive

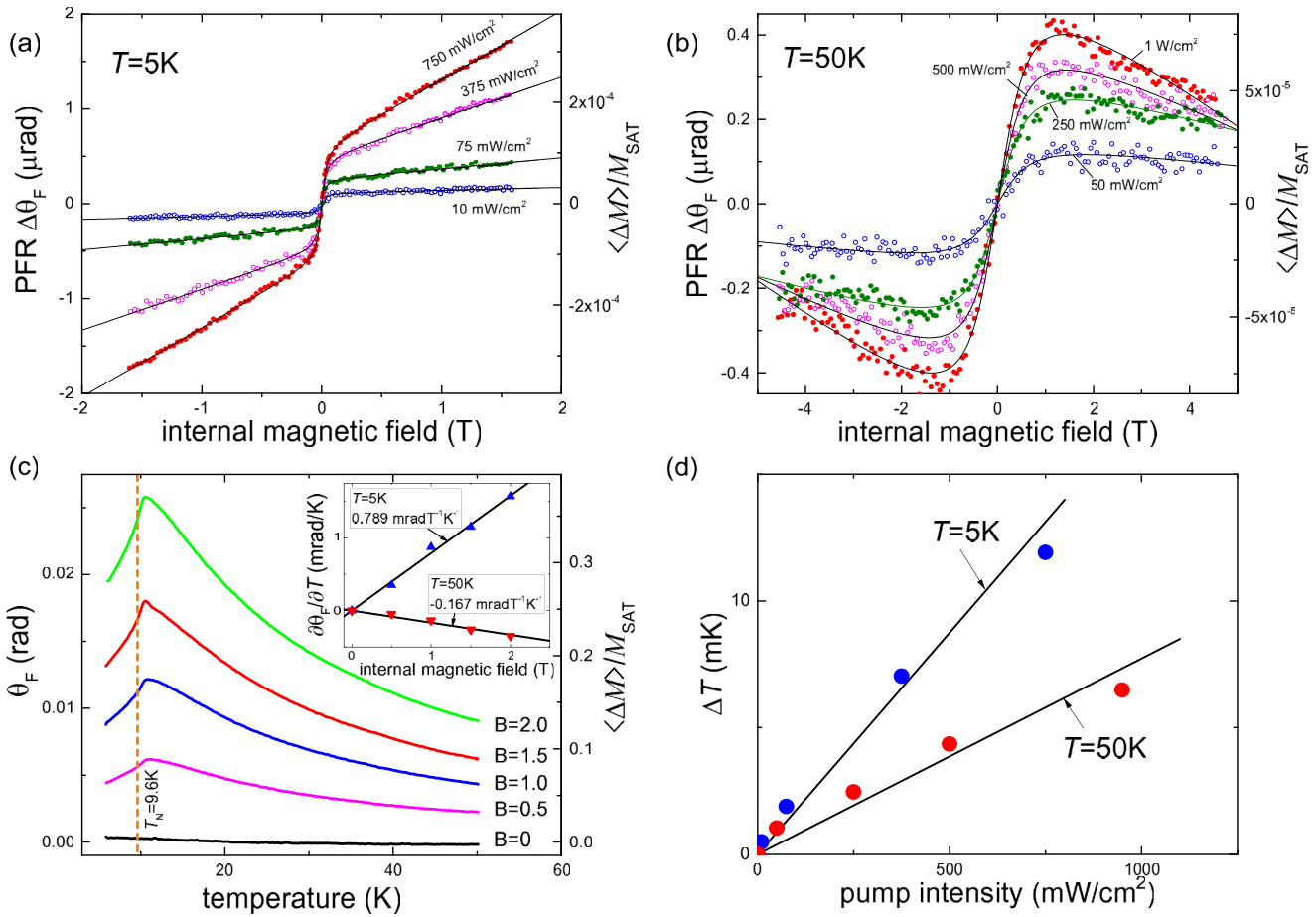


FIG. 3. (a) Photoinduced Faraday rotation at 5 K and (b) at 50 K. (c) Faraday rotation by the bulk EuTe sample as a function of temperature for various magnetic fields. (Notice that for our sample the observed Néel temperature is slightly larger than the accepted value of 9.6 K for EuTe, in agreement with direct measurements reported in Ref. [13]). The slope of the dependance of  $\partial\theta_F/\partial T$  on  $B$  is shown in the inset. (d) The deduced temperature modulation of the illuminated region is shown as a function of the pump intensity for  $T = 5\text{ K}$  and  $T = 50\text{ K}$ .

to negative when we cross the Néel temperature. This is exactly what we observe, as can be seen from Fig. 3(a) for  $T = 5\text{ K}$ , where the thermal background has a positive slope, and Fig. 3(b) for  $T = 50\text{ K}$ , where the slope of the background signal is negative. The temperature modulation at  $T = 50\text{ K}$  was found by using Eq. (12), and it is also shown in Fig. 3(d). At 50 K the heating effect is smaller than at 5 K due to a larger heat capacity of the EuTe crystal [21]. Another aspect worthy of comment is that, upon closer inspection of Fig. 3(d), the temperature modulation  $\Delta T$  presents a slightly sublinear dependence on pump intensity. This can be attributed to the fact that, for a larger excitation power, the effective volume excited by light increases, because the threshold excitation light penetrates deeper into the sample. In this case, the temperature increase for doubled excitation power will obviously be less than doubled, which explains the sublinear behavior of  $\Delta T$  on the excitation power.

Having subtracted the linear thermal background from the  $\Delta\theta_F$  vs  $B$  curves, as deduced above, the saturation polaron magnetization  $\Delta\theta_F^{\text{SAT}}$  for every pump intensity was extracted and it is plotted in Fig. 4.  $\Delta\theta_F^{\text{SAT}}$  increases sublinearly with pump intensity, indicating that polarons are less and less efficiently generated when the pump intensity is increased.

Taking into account that optical absorption leads to an exponentially decreasing pump intensity below the surface of

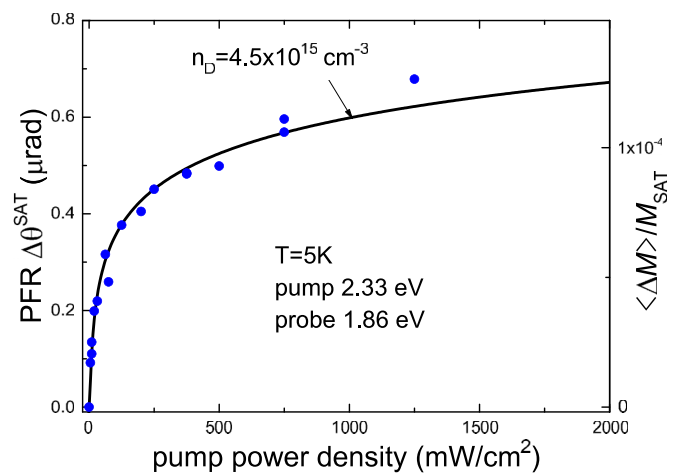


FIG. 4. Dots show the photoinduced Faraday rotation angle at saturation as a function of the pump intensity. The full line shows a fit of the dots with Eq. (14), which yields the maximum polaron concentration to be  $n_D = 4.5 \times 10^{15}\text{ cm}^{-3}$ .

the sample, then the concentration of photogenerated polarons at a depth  $x$  below the surface will be

$$n_{\text{Pol}}(x) = \chi \frac{pe^{-\alpha x}}{h\nu} \tau_0. \quad (13)$$

We shall assume, however, that the concentration of polarons that can be generated is limited by a maximum value, represented by  $n_D$ . Then the photoinduced Faraday rotation in the saturated fields will be given by

$$\begin{aligned} \Delta\theta_F^{\text{SAT}} &\sim \int_0^\infty n_{\text{Pol}}(x) dx \\ &= \frac{n_D}{\alpha} \begin{cases} \frac{p}{p_D} & \text{if } p < p_D \\ (1 + \ln \frac{p}{p_D}) & \text{if } p > p_D, \end{cases} \end{aligned} \quad (14)$$

where  $p_D = \frac{n_D h\nu}{\chi \alpha \tau_0}$ . Equation (14) gives a photoinduced Faraday rotation angle that increases linearly with pump intensity for  $p < p_D$  and logarithmically for  $p > p_D$ . Figure 4 shows that Eq. (14) provides a very good fit of our data, whereby  $n_D$  is the single adjustable parameter, yielding  $n_D = 4.5 \times 10^{15} \text{ cm}^{-3}$ . This is again far less than the concentration of polarons that would completely fill the excited layer,  $(\frac{4}{3}\pi R_{\text{Pol}}^3)^{-1} = 1.3 \times 10^{19} \text{ cm}^{-3}$ . We attribute the limited concentration of polarons that can be photogenerated to their binding by residual defects of concentration  $n_D$ . At  $T = 5 \text{ K}$ , these bound polarons are long-lived—their lifetime is  $15 \mu\text{s}$  [7]—and therefore have a supremacy over magnetic polarons seen in the photoluminescence, which have a much shorter lifetime, of the order of a nanosecond [22]. The shorter lifetime implies a stationary concentration of magnetic polarons that is four orders of magnitude smaller, and effectively only the long-lived magnetic polarons will be observed in the photoinduced Faraday rotation. A plausible source of defects at a low concentration of the order of  $10^{15} \text{ cm}^{-3}$  is the unbalanced stoichiometry of the Eu and Te atomic fluxes during the MBE growth. It should be observed that the binding of polarons to defects provides further support for our previous assumption that photoexcited polarons remain localized in the penetration layer of the pump light and do not diffuse into the interior of the EuTe crystal.

Equation (7) can be rewritten as

$$\Delta\theta_F(B, T) = \Delta\theta_F^{\text{SAT}}(T) L\left(\frac{\mu_{\text{Pol}} B}{k_B T}\right), \quad (15)$$

where  $\Delta\theta_F(B, T)$  is the photoinduced Faraday rotation at a field  $B$  and a temperature  $T$ , and  $\Delta\theta_F^{\text{SAT}}(T)$  is the corresponding saturation value, depicted in Fig. 2. The measured data for various temperatures was fitted with Eq. (15), yielding two parameters for each temperature: the magnetic moment of the photoinduced magnetic polaron,  $\mu_{\text{Pol}}(T)$ , and the Faraday rotation step height when  $B$  is varied,  $\Delta\theta_F^{\text{SAT}}(T)$  (see Fig. 2). It is worth pointing out that the polaron magnetic moment is the only parameter defining the smoothness of the step, so the value for  $\mu_{\text{Pol}}$  obtained from the fit is independent of any other parameter entering Eq. (15), such as the polaron lifetime and steady-state population, which depend on temperature. Figure 5(a) shows the polaron magnetic moment as a function of temperature so obtained. For comparison, the dashed line in Fig. 5(a) is given by the magnetic moment associated with

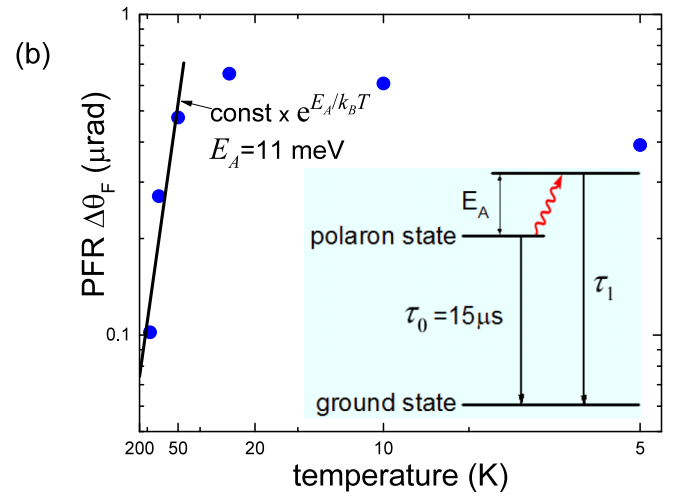
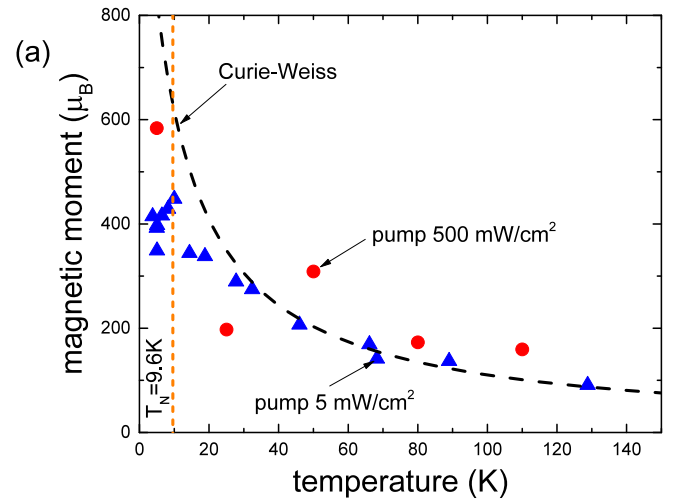


FIG. 5. (a) Temperature dependence of the magnetic moment of a polaron. (b) Temperature dependence of the photoinduced Faraday rotation angle at saturation. Above  $T \sim 50 \text{ K}$ ,  $\Delta\theta_F^{\text{SAT}}$  decreases exponentially with a characteristic activation energy of  $E_A = 11 \text{ meV}$ . The inset shows schematically the magnetic polaron energy level, the ground state (when the photoexcited electron is absent), and the thermally activated state, which drains the polaron population when the temperature of the sample is increased.

the polaron sphere

$$\mu_{\text{Pol}} = \frac{4}{3}\pi R_{\text{Pol}}^3 \langle M \rangle, \quad (16)$$

where  $\langle M \rangle$  is the average EuTe magnetization within the magnetic polaron sphere under the action of the exchange field of the photoexcited electron,  $B_{\text{Xf}} \approx 1 \text{ T}$  [5,6], taken in the Curie–Weiss approximation [18]

$$\langle M \rangle = n_{\text{Eu}} \mu_{\text{Eu}} \frac{g \mu_B (S + 1)}{3k_B} \frac{B_{\text{Xf}}}{T + T_N}.$$

It can be seen that the Curie–Weiss law describes the data quite well, without any adjustable parameter.

Finally, Fig. 5(b) shows a plot of the second parameter obtained from the fit, i.e., the photoinduced Faraday rotation at the saturation level,  $\Delta\theta_F^{\text{SAT}}(T)$ , as a function of temperature. Above  $100 \text{ K}$ , the photoinduced Faraday rotation decreases exponentially with an activation energy

of about 11 meV. The rapid decrease of the photoinduced Faraday rotation signal is interpreted in terms of the thermal activation of a fast recombination channel, which causes a reduction of the polaron lifetime and hence of the steady-state polaron population. The thermally activated magnetic polaron quenching process is illustrated by the energy-level scheme shown in the inset of Fig. 5(b).

In conclusion, we have shown that EuTe can be magnetized by light through optical generation of magnetic polarons, with a quantum efficiency of  $\chi \sim 0.09$  and a maximum concentration, which is about  $4.5 \times 10^{15} \text{ cm}^{-3}$  in the case of the sample studied in this work. Such a low concentration is evidence that the magnetic polarons are bound to defects, plausibly generated during the growth process due to a deviation from stoichiometry. A path to clarify this point would be to investigate samples with an intentional deviation from stoichiometry and check if the deviation correlates with the

maximum polaron concentration. At low temperatures, the polarons are immobile and do not diffuse out of the illuminated volume. The polaron population can be thermally quenched, with an activation energy of 11 meV, which could be due to thermally activated recombination, or to polaron diffusion out of the path of the probe beam. Thus, we demonstrated a novel approach for the optical manipulation of magnetic states in EuTe, which in principle should be valid for any intrinsic magnetic semiconductor, as well as for diluted semiconductors and for hybrid ferromagnetic-semiconductor structures.

This work was supported by the Brazilian agency CNPq (Projects 401694/2012-7, 307400/2014-0, and 456188/2014-2) and by the Ministry of Education and Science of the Russian Federation (Project ID RFMEF161315X0048/14.613.21.0048). A.R.N. was supported by a fellowship from CAPES-Brazil.

- 
- [1] A. Kirilyuk, A. V. Kimel, and T. Rasing, *Rev. Mod. Phys.* **82**, 2731 (2010).
- [2] T. Makino, F. Liu, T. Yamasaki, Y. Kozuka, K. Ueno, A. Tsukazaki, T. Fukumura, Y. Kong, and M. Kawasaki, *Phys. Rev. B* **86**, 064403 (2012).
- [3] M. Matsubara, A. Schroer, A. Schmehl, A. Melville, C. Becher, M. Trujillo-Martinez, D. G. Schlom, J. Mannhart, J. Kroha, *et al.*, *Nat. Commun.* **6**, 6724 (2015).
- [4] R. R. Subkhangulov, A. B. Henriques, P. H. O. Rappl, E. Abramof, T. Rasing, and A. V. Kimel, *Sci. Rep.* **4**, 4368 (2013).
- [5] A. B. Henriques, G. D. Galgano, E. Abramof, B. Diaz, and P. H. O. Rappl, *Appl. Phys. Lett.* **99**, 091906 (2011).
- [6] A. B. Henriques, F. C. D. Moraes, G. D. Galgano, A. J. Meaney, P. C. M. Christianen, J. C. Maan, E. Abramof, and P. H. O. Rappl, *Phys. Rev. B* **90**, 165202 (2014).
- [7] A. B. Henriques, G. D. Galgano, P. H. O. Rappl, and E. Abramof, *Phys. Rev. B* **93**, 201201(R) (2016).
- [8] T. Dietl, *Acta Phys. Pol.* **94**, 111 (1998).
- [9] *Introduction to the Physics of Diluted Magnetic Semiconductors*, edited by J. Kossut and J. A. Gaj, Springer Series in Materials Science (Springer, Berlin, Heidelberg, 2010).
- [10] T. Kasuya, A. Yanase, and T. Takeda, *Solid State Commun.* **8**, 1543 (1970).
- [11] E. L. Nagaev, *Phys. Status Solidi B* **145**, 11 (1988).
- [12] A. Mauger and D. L. Mills, *Phys. Rev. B* **31**, 8024 (1985).
- [13] B. Díaz, E. Granado, E. Abramof, P. H. O. Rappl, V. A. Chitta, and A. B. Henriques, *Phys. Rev. B* **78**, 134423 (2008).
- [14] C.-Y. Chang, L. Wang, J.-T. Shy, C.-E. Lin, and C. Chou, *Rev. Sci. Instrum.* **82**, 063112 (2011).
- [15] A. Mauger and C. Godart, *Phys. Rep.* **141**, 51 (1986).
- [16] L. K. Hanamoto, A. B. Henriques, N. F. Oliveira, P. Rappl, E. Abramof, and Y. Ueta, *J. Phys.: Condens. Matter* **16**, 5597 (2004).
- [17] A. B. Henriques, A. Wierth, M. A. Manfrini, G. Springholz, P. H. O. Rappl, E. Abramof, and A. Y. Ueta, *Phys. Rev. B* **72**, 155337 (2005).
- [18] S. Blundell, *Magnetism in Condensed Matter* (Oxford University Press, Oxford, UK, 2001).
- [19] R. T. Lechner, G. Springholz, T. U. Schüllli, J. Stangl, T. Schwarzl, and G. Bauer, *Phys. Rev. Lett.* **94**, 157201 (2005).
- [20] N. F. Mott, in *Metal-Insulator Transitions*, 2nd ed., Springer Series in Materials Science (Taylor & Francis, London, 1990), p. 93.
- [21] I. A. Smirnov, *Phys. Status Solidi A* **14**, 363 (1972).
- [22] W. Heiss, R. Kirchschrager, G. Springholz, Z. Chen, M. Debnath, and Y. Oka, *Phys. Rev. B* **70**, 035209 (2004).